Fermi National Accelerator Laboratory

FERMILAB-Pub-91/94-T

DURHAM DTP-91/20

May, 1991

Approximating the Production of a Vector Boson plus Multi-Jets at Hadron Colliders

C. J. MAXWELL

Department of Physics,

University of Durham, Durham U.K.

and

Stephen PARKE

Fermi National Accelerator Laboratory [1]

P.O. Box 500, Batavia, IL 60510.

Abstract

We give approximations to the matrix element squared for the production of a vector boson accompanied by an arbitrary number of jets. Only subprocesses containing one and two quark-antiquark pairs are estimated. Approximate cross sections and kinematical distributions are compared to those obtained from the known exact tree level matrix elements for W plus four and three jets and Z plus three jets using all subprocesses and an agreement at the $\sim 30\%$ level is found. The approximations are simple and can be rapidly evaluated on a computer, saving an order of magnitude in CPU time compared to using the tree level exact matrix elements. Estimates of the W plus five jets and the Z plus four jet cross sections as well as their kinematical distributions are also given.

Operated by Universities Research Association Inc. under contract with the United States Department of Energy

1 Introduction

Processes in which a vector boson is produced in association with jets will provide important backgrounds in searches for the top quarks and the Higgs boson at hadron colliders. The W boson plus four jet case has recently received particular attention in this regard[1].

The exact tree-level QCD matrix elements for processes with a W boson and up to six partons (i.e. four final state jets) are now available[1],[2],[3]. For W plus four jet production the number of contributing processes and the complexity of the exact matrix elements means that a large amount of computer CPU time is required for Monte Carlo simulations of events. (52 sec CPU/event on a VAX 780 for W + 4 jets using the simulations of ref. [1]). Since for background estimates one would like to produce rather high statistics simulations, experimenting with the kinematical cuts, it would be useful to have approximations to the matrix elements available which are accurate at the 20-30% level point-by-point in phase space, and which reduce the CPU time needed by an order of magnitude.

In this paper we shall explicitly construct and test such approximations. In Section II we shall briefly review the approximation technique, the 'infra-red reduction' scheme introduced in ref.[4]. Section III will detail the application to vector boson plus jets production, and Section IV will present comparisons of the approximate results with those obtained using the exact tree level matrix elements. Section V will contain our conclusions.

2 The 'Infra-red Reduction' Technique

The basis of the approximations is the 'infra-red reduction' procedure introduced for approximating multi-gluon scattering in ref. [4], and subsequently extended to $q\bar{q}$ +

gluons [5],[6] and $e^+e^-q\bar{q}$ + gluons in ref. [7]. The idea is to approximate the matrix element squared for some QCD process with n final partons $|M_n|^2$, by writing

$$|M_n|^2 \;=\; \left\{\frac{|M_n|^2}{|M_n^S|^2}\right\} \;\; |M_n^S|^2. \tag{2.1}$$

$|M_n^S|^2$ can be any simple function of four-momenta which has the same soft and collinear kinematical poles as $|M_n|^2$. In this way the bracketed ratio in eqn(2.1) will be finite even for collinear configurations where $|M_n|^2$ itself is singular. To approximate $|M_n|^2$ for some momentum configuration, presumably with energetic well-separated partons, one then approximates the ratio by evaluating it at some 'nearby' configuration where two of the final partons are collinear. For such configurations the ratio can be obtained using the Altarelli-Parisi behavior of the full amplitude. The remaining factor of $|M_n^S|^2$ is evaluated using the original momentum configuration.

There is no unique Lorentz invariant way to define this 'nearby' configuration. A method which is simple and seems to work well in practice [4]-[7], is to replace the pair of final partons having the smallest invariant mass $(p_i \,+\, p_j)^2$ by a collinear pair in the direction of $\vec{p_i} \,+\, \vec{p_j}$ with energy factions $z = E_i/(E_i \,+\, E_j)$ and $1-z$. Here E_i, E_j, $\vec{p_i}$, $\vec{p_j}$ are the energies and three-momenta in the centre of mass frame of the incoming particles.

Denoting $(p_i \,+\, p_j)^2 \equiv 2(p_i \,\cdot\, p_j)$ by the shorthand (ij) we have in this collinear limit[8]

$$\lim_{(ij)\,\to\,0} (ij)\; |M_n|^2 \;=\; 2g^2\; P_{ij}(z)\; |M_{n-1}|^2. \tag{2.2}$$

The limit is taken such that for some final pair of partons i and j, $p_i \;\to\; z\; p_a$ and $p_j \;\to\; (1-z)\; p_a$ with $p_a \;=\; p_i \,+\, p_j$. g is the strong coupling 'constant' $(\alpha_s \;=\; \frac{g^2}{4\pi})$ and $P_{ij}(z)$ are the Altarelli-Parisi splitting kernels. For a gluon pair going collinear $ij \;=\; gg$, for a quark and a gluon $ij \;=\; qg$ or gq, and for a quark and antiquark $ij \;=\; q\bar{q}$.

The simple amplitude $|M_n^S|^2$ will have some calculable behaviour in the collinear limit

$$\lim_{(ij)\,\to\,0} (ij)\; |M_n^S|^2 \;=\; 2g^2\; \tilde{P}_{ij}(R,z)\; |M_{n-1}^S|^2, \tag{2.3}$$

where R denotes the residual kinematics, with one fewer momentum, remaining after the reduction.

The bracketed ratio of amplitudes in eqn(2.1) can then be approximated at this collinear configuration by

$$\frac{|M_n|^2}{|M_n^S|^2} \simeq \frac{|M_n|^2}{|M_n^S|^2}|_{collinear} = F_{ij}(R,z) \ \frac{|M_{n-1}|^2}{|M_{n-1}^S|^2} \tag{2.4}$$

where we have defined

$$F_{ij}(R,z) \equiv \frac{P_{ij}(z)}{\bar{P}_{ij}(R,z)}. \tag{2.5}$$

By using this approximation recursively $(n-m)$ times one arrives at

$$|M_n|^2 \simeq \Pi_{i=1}^{n-m} \ F^i(R,z) \, \frac{|M_m|^2}{|M_m^S|^2} \ |M_n^S|^2 \tag{2.6}$$

The formalism can be trivially extended to the case where the minimum dot product involves an initial and a final momentum. Defining $z = E_i/(E_i + E_j)$ the same expressions apply, but now z cannot be directly interpreted as the energy fraction since if 'i' is an initial particle one has $z > 1$, since $E_i < 0$.

An obvious question concerns the best choice for $|M_n^S|^2$. One may identify two requirements which will tend to produce a good approximation. The function $F(R,z)$ of eqn(2.5) should be insensitive to the value of z and to the residual kinematics, and the final ratio $|M_m|^2/|M_m^S|^2$ in eqn(2.6) should also be insensitive to the kinematics.

For the processes to which the approximation has been so far applied it is possible to write for one helicity amplitude (the most helicity violating nonzero amplitude), a simple expression for the matrix element squared for an arbitrary number of partons, exact to leading order in the number of colors. This expression is an obvious candidate for $|M_n^S|^2$. In the multi-gluon case the special expression is the Parke-Taylor matrix element[9], for $q\bar{q}+$ gluons and $e^+e^-q\bar{q}+$ gluons processes similar results exist[10]–[13]. For all of these cases the corresponding $F(R,z)$ is smoothly behaved. For instance for multi-gluon scattering $1 \leq F_{gg}(R,z) \leq 2$, see [6], and for $e^+e^- q\bar{q}$ + gluons $F_{gg}(R,z) = z^4 + (1-z)^4 + 1$, see [7], which is evidently not strongly dependent on z, and does not in fact depend on the residual kinematics. Furthermore for $gg \to ggg$ and $e^+e^- \to q\bar{q}g$ (or crossings) these special formulae are exact, and so if one reduces $(n-3)$ times the final factor of $|M_3|^2/|M_3^S|^2$ is unity. Since the F factors are close to unity, the most helicity violating amplitudes dominate, and the approximation is estimating the full amplitude by adjusting this dominant helicity amplitude with a smoothly behaved correction factor. The approximations work well point-by-point in phase space, guaranteeing that the shape and normalization of the distributions are well reproduced at the $\sim 20\%$ level [4]-[7].

For multi-gluon scattering, $q\bar{q}+$ gluons and $e^+e^- q\bar{q}+$ gluons there exist recursive relations based on the Berends-Giele recursion relations [1],[11] which enables these processes to be evaluated exactly, at tree level, for any number of partons. The CPU time required for these computations rapidly grows very large, however, making going beyond $2 \to 5$ in multi-gluon and $q\bar{q}+$ gluons scattering very time consuming; $2 \to 6$ is the corresponding feasible limit for $e^+e^- q\bar{q}+$ gluons. The infrared reduction technique enables one to flexibly approximate, trading off time against accuracy. For instance to approximate $2 \to 6$ multigluon scattering one could perform one reduction and use eqn(2.6) with the exact $2 \to 5$ result, or one could perform two reductions and use the exact $2 \to 4$ result.

Each extra reduction represents an extra approximation and hence a loss of accuracy, but the exact result needs to be evaluated for fewer particles and hence can be evaluated faster. In practice the degradation in accuracy with increasing number of reductions is rather mild.

A further advantage of the technique is that it can be used in cases where no analogue of the Parke-Taylor matrix element exists. One can guess an $|M_n^S|^2$ with the correct soft and collinear pole structure, and providing the $F(R,z)$'s do not have a strong R and z

dependence the approximation is likely to work well. In a recent application, ref.[14], the six jet QCD background to top decay involving a $b\bar{b}$ pair has been estimated taking $|M_n^S|^2$ as the Parke-Taylor matrix element. We now turn to the construction of such approximations for a vector boson (W or Z) plus multi-jet production.

3 Approximating Vector Boson plus Multi-jet Production

We shall mainly concentrate on $W^\pm$ plus multi-jet production here, since this process has greater present relevance for background calculations in $t\bar{t}$ production. We shall consider two classes of subprocesses - $W^\pm q\bar{q}' +$ gluons and $W^\pm p\bar{p}'q\bar{q} +$ gluons, containing one and two quark-antiquark pairs respectively. We shall not attempt to approximate the subprocesses with three quark-antiquark pairs since these make only a small contribution to the cross section, at least for the $W^\pm$ + four final jets case where they have been calculated [1].

For the $W^\pm q\bar{q}' +$ gluons subprocesses there exists an analogue of the Parke-Taylor matrix element for the helicity amplitude where all the gluon helicities are the same. If we allow the $W^\pm$ to decay into a lepton-antilepton pair, $l\bar{l}'$, then for the $l\bar{l}'q\bar{q}'\ g_1 \ldots g_n$ subprocess, one has to leading order in N_c [11]-[13],

$$\begin{aligned}
|M_n^{S\pm}|^2 &= N_c^{n-1}(N_c^2-1)\ A_\pm(l,\bar{l}',q,\bar{q}') \\
&\quad \times \frac{(l\bar{l}')}{[(W^2-M_W^2)^2\ +\ M_W^2\Gamma_W^2]} \\
&\quad \times \sum_P \frac{1}{(qg_1)(g_1g_2)\cdots(g_{n-1}g_n)(g_n\bar{q}')},
\end{aligned} \tag{3.1}$$

the $\pm$ indicating $W^\pm$ production with

$$A_+(l,\bar{l}',q,\bar{q}') = [(lq)^2 + (\bar{l}'\bar{q}')^2]$$
$$A_-(l,\bar{l}',q,\bar{q}') = [(l\bar{q}')^2 + (\bar{l}'q)^2]. \tag{3.2}$$

The 'P' denotes a sum over all n! permutations of the gluon momenta. We have set weak and strong coupling constants to unity and omitted the averaging factors which depend on the crossing. All particles are assumed outgoing, and we use the particle letter to stand for their four-momenta. The expression eqn(3.1) can be used for all the independent crossings, i.e. $q\bar{q}' \rightarrow l\bar{l}'g\ldots$ or $gq \rightarrow l\bar{l}'q'g\ldots$ or $gg \rightarrow l\bar{l}'q\bar{q}'g\ldots$.

We may note that the $A_\pm$ factors introduce a strong angular correlation between the quark and lepton directions. This correlation is not present in the full squared amplitude for the subprocess. We therefore choose to construct our approximation by replacing $A_\pm$ by the average, $A = (A_+ + A_-)/2$. Then for both W^+ and W^- we use as $|M_n^S|^2$,

$$|M_n^S|^2 = N_c^{n-1}(N_c^2-1)A(l,\bar{l}',q,\bar{q}') \times \frac{(l\bar{l}')}{[(W^2-M_W^2) + M_W^2\Gamma_W^2]} \times \sum_P \frac{1}{(qg_1)(g_1g_2)\cdots(g_{n-1}g_n)(g_n\bar{q}')}. \tag{3.3}$$

Of course the corresponding exact $|M_n^\pm|^2$ will differ for $W^\pm$.

The F factors of eqn(2.5) corresponding to eqn(3.3) are then,

$$F_{gg}(R,z) = z^4 + (1-z)^4 + 1$$
$$F_{qg}(R,z) = \frac{8}{9}\frac{(1+R)(1+z^2)}{(R+z^2)} \tag{3.4}$$

for $g \parallel g$ and $q \parallel g$ reduction respectively with

$$R = \frac{(l\bar{q}')^2 + (\bar{l}'\bar{q}')^2}{(lq_a)^2 + (\bar{l}'q_a)^2} \tag{3.5}$$

for $q \parallel g$ reduction, $q_a \equiv q + g$. For $\bar{q}' \parallel g$, $q \leftrightarrow \bar{q}'$ and $q_a \equiv \bar{q}' + g$.

In ref.[6] a trivial modification to the infra-red reduction procedure was proposed so that the reduced set of momenta are on-shell (i.e. massless, since we are assuming massless partons). One simply replaces the pair of final state partons i, j with the smallest invariant mass (ij) by the momentum

$$p_a = (|\vec{p_i} \ + \ \vec{p_j}| \ , \ \vec{p_i} \ + \ \vec{p_j}) \tag{3.6}$$

where the $\vec{p_i}$'s are the three-momenta in the centre of mass frame of the incoming particles. Momentum conservation will still hold but energy conservation will be violated. To restore it one can simply multiply all the final four-momenta by a factor

$$\lambda \ = \ \frac{\sqrt{\hat{s}}}{\sum_{k \ final} E_k} \tag{3.7}$$

where the sum over final energies includes $E_a \ = \ |\vec{p_i} \ + \ \vec{p_j}|$ and $\sqrt{\hat{s}}$ denotes the total subprocess centre of mass energy. The triangle inequality guarantees $\lambda \geq 1$, since $|\vec{p_i} \ + \ \vec{p_j}| \leq |\vec{p_i}| \ + \ |\vec{p_j}|$ and hence $E_a \leq E_i \ + \ E_j$ (with equality only if $(ij) = 0$). For our present purposes such a rescaling of the lepton and antilepton momenta would correspond to a W mass increase by a factor of λ^2, which is evidently rather undesirable. We therefore prefer to restore energy conservation by multiplying the initial momenta by a factor $\frac{1}{\lambda} \leq 1$, which corresponds to a slightly reduced $\sqrt{\hat{s}}$, but an unaltered M_W. In principle one could also modify the algorithm for initial/final reduction proposed in [6] to similarly preserve M_W. Since for realistic E_T and ΔR cuts the minimum invariant mass pair are almost always final state, and since the initial/final algorithm is rather unstable, we shall construct our vector boson plus multi-jet approximations by reducing on the final state partons only, using the modified algorithm above.

We now turn to the problem of approximating the subprocesses with two quark-antiquark pairs. Here, unfortunately we do not have such a well defined starting point, since there does not exist an analogue of the Parke-Taylor matrix elements. The amplitude squared for the process $p\bar{p}q\bar{q}g_1 \ldots g_n$, with all the gluons having the same helicity, to leading order in N_c, is [13]

$$|M_n^{S2}|^2 = N_c^n(N_c^2-1)\,\frac{A_0(p,\bar{p},q,\bar{q})}{(\bar{q}q)(\bar{p}p)} \times \sum_P \frac{(p\bar{q})}{(pg_1)\cdots(g_k\bar{q})}\;\frac{(q\bar{p})}{(qg_{k+1})\cdots(g_n\bar{p})}. \tag{3.8}$$

Coupling constants are set to unity and averaging factors omitted as before. 'P' denotes a sum over all partitions of the n gluons into two subsets with k in one and $n-k$ in the other with all permutations of the gluons within these partitions, and

$$A_0(p,\bar{p},q,\bar{q}) = [(pq)^2 + (p\bar{q})^2 + (\bar{p}q)^2 + (\bar{p}\bar{q})^2]. \tag{3.9}$$

If we allow a photon to radiate from the $p\bar{p}$ quark line then this matrix element squared is multiplied by

$$\frac{(p\bar{p})}{(p\gamma)(\gamma\bar{p})}. \tag{3.10}$$

This is the factor for independent radiation along this quark line. Guessing that we can replace the photon by a W boson and allow the W to decay, we arrive at a choice for $|M_n^{S2}|^2$ for the $l\bar{l}'p\bar{p}'q\bar{q}\;g_1\ldots g_n$ process of

$$\begin{aligned}|M_n^{S2}|^2 &= N_c^n(N_c^2-1)\frac{A_0(p,\bar{p}',q,\bar{q})}{(\bar{q}q)[(p + l + \bar{l}')^2][(\bar{p}' + l + \bar{l}')^2]} \\ &\times \frac{(l\bar{l}')}{[(W^2-M_W^2)^2 + M_W^2\Gamma_W^2]} \\ &\times \sum_P \frac{(p\bar{q})}{(pg_1)\cdots(g_k\bar{q})}\;\frac{(q\bar{p}')}{(qg_{k+1})\cdots(g_n\bar{p}')}.\end{aligned} \tag{3.11}$$

with A_0 given by eqn(3.9). For the subprocesses in which a quark or antiquark flavor is repeated we simply add extra terms to eqn(3.11) with $p \leftrightarrow q$ or $\bar{p}' \leftrightarrow \bar{q}$.

The $F(R,z)$ factor corresponding to eqn(3.11) for $g \parallel g$ reduction is

$$F_{gg} = z^4 + (1-z)^4 + 1. \tag{3.12}$$

This is the same well-behaved factor one finds for the single $q\bar{q}'$ pair process, eqn(3.4). The factor F_{qg} with the above choice is rather messy and so we shall reduce on the pair of final gluons only in the approximating the $l\bar{l}'p\bar{p}'q\bar{q}+$ gluons subprocesses. For W plus four final state jets there is at maximum one final gluon pair, and this means that we cannot approximate the crossings of this process containing initial gluons. Fortunately these crossings contribute only some 20% of the total two quark-antiquark pair contribution, and so their neglect is not important.

So far we have concentrated on W + multijet production. We can, however, use the above results to approximate Z^0 + multijet production. The $Z^0 q\bar{q}+$ gluons subprocesses ($l\bar{l}q\bar{q}$ + gluons) can be approximated using the $|M_n^S|^2$ of eq.(3.3), with the obvious replacement of $\bar{l}'$ by $\bar{l}$, $\bar{q}'$ by $\bar{q}$, and W, M_W, Γ_W by Z, M_Z, and Γ_Z. Similar replacements applied to eq.(3.11) provide a basis for approximating $Z^0 p\bar{p}q\bar{q}+$ gluons,we need to add to (3.11) the terms with $(p,\bar{p})$ interchanged with $(q,\bar{q})$.

We now turn to comparisons of these approximations with the exact tree level results for producing a vector boson and up to four final jets.

4 Testing the Approximations

In this section we shall compare the approximations of Section III with the exact tree level results based on the matrix elements of ref. [1]. We have smeared over the vector boson width for both the approximate and exact calculations. We shall use MRSED structure functions [15] and choose $Q^2 = M_W^2$ as the scale in the one-loop QCD running α_s. We take $\Lambda_{\overline{MS}} = 200 MeV$.

We begin by testing the performance of the approximations for the $W^\pm q\bar{q}'+$ gluons subprocesses. We use the standard cuts for the FNAL Tevatron and the SSC as given in Table 1. With these cuts and choices the performance of the approximation versus the exact result is summarized for W plus four jet production (approximated with one reduction to W plus three jets) in Table 2, and W plus three jet production (approximated with one reduction to W plus two jets) in Table 3.

In these tables f_{30}, f_{20}, f_{10} denote the fraction of generated phase space points passing the cuts for which the approximate and exact weights are within 30%, 20%, 10% respectively. σ_{app} and σ_{ex} denote the approximate and tree level cross sections. The uncertainties quoted are those of the numerical integration. Only those crossings with at least one initial quark or antiquark for the $W^{\pm}q\bar{q}' +$ gluons subprocesses are considered and final/final reductions only are applied. As can be seen from the Tables the approximation performs very well for both W + 4 jets and W + 3 jets at both Fermilab and SSC energies. For W plus four jets, 72% of the points have the exact and approximate weights within 30%. The integrated σ_{app} is within 10% of σ_{ex}.

For the $W^{\pm}q\bar{q}' +$ gluons subprocesses we plot various kinematical distributions for $W + 4$ jets and $W + 3$ jet production at $\sqrt{s} = 1.8 TeV$ in Figs 1,2. The histograms (a)-(f) give, respectively, the E_T of the jets, the jet pseudorapidity, W transverse momentum, W plus one jet mass, W plus all jet mass, all jet mass distributions. The solid line corresponds to the exact matrix element and the points are the approximate matrix element. Within statistics there is evidently good agreement for all these distributions. We have checked that the agreement is correspondingly good at $\sqrt{s} = 40 TeV$.

We next perform similar comparisons for the $W^{\pm}p\bar{p}'q\bar{q}$ + gluons subprocesses for W + 4 jet production (approximated by reduction to W + 3 jets). We cannot approximate W + 3 jets using only $g \parallel g$ reductions, as proposed in section III, since there is at most only one gluon in the final state. In Table 4 the performance of the approximation is shown. Once again the approximation works well at both energies, with f_{30} greater than 70%. Given the other uncertainties in a tree-level evaluation this level of performance is quite acceptable.

In Figs 3(a)-(f) we plot the approximate and exact histograms for the $W^{\pm}p\bar{p}'q\bar{q}gg$, W + 4 jet subprocesses at $\sqrt{s} = 1.8 TeV$. There is good agreement within statistics.

We have checked that the performance is comparably good at $\sqrt{s} = 40TeV$.

Finally we give in Fig. 4(a)-(f) the overall approximate verses exact histograms for $W + 4$ jets at $\sqrt{s} = 1.8TeV$, where all subprocesses including W plus three quark-antiquark pairs have been included in the exact cross section and the approximation involves only the one and two quark-antiquark pair subprocesses (with one reduction to $W + 3$ jets). The all subprocess cross section result is $\sigma_{ex} = 0.79 \pm 0.04\ pb$ and $\sigma_{app} = 0.60 \pm 0.04\ pb$ at $\sqrt{s} = 1.8TeV$. At $\sqrt{s} = 40TeV$ we find $\sigma_{ex} = 46 \pm 4\ pb$ and $\sigma_{app} = 43 \pm 4\ pb$. The VAX 780 CPU time/event is 52 sec for the exact matrix element and 2.3 sec for the approximations.

Exact tree level matrix elements for W+5jet production have yet to be calculated. We give in Fig. 5(a)-(f) the approximate W + 5 jet predictions obtained by performing one reduction and using the exact W + 4 jet matrix elements (solid line), one and two $q\bar{q}$ pair subprocesses are considered, three $q\bar{q}$ pair processes being neglected as before. The points indicate the results obtained performing two reductions and using the exact W + 3 jet matrix elements. There is evidently good agreement. The exact W + 3 jet matrix elements are much faster to evaluate (23 sec of VAX 780 CPU time/event for 1 reduction, compared to 2.5 sec VAX 780 CPU time/event for two reductions). The total W + 5 jet cross sections obtained for one and two reductions respectively are $\sigma^1_{app} = 0.074 \pm 0.003pb$ and $\sigma^2_{app} = 0.064 \pm 0.003pb$

We finally perform some comparisons of approximate versus exact results for Z + jet production. Exact tree level matrix elements for up to three jets only are available [1]. We have compared the approximate with exact Z + 3 jet results for the $Z^0 q\bar{q}ggg$ subprocesses. The level of agreement is good and very similar to that obtained for W + 3 jets in Table 4. At $\sqrt{s} = 1.8$ TeV we have $\sigma_{ex} = 0.18 \pm 0.01$pb versus $\sigma_{app} = 0.15 \pm 0.01$pb We give in Fig. 6(a)-(f) approximate histograms for Z + 4 jets including one and two $q\bar{q}$ pair processes as before. We perform one reduction and use the exact Z + 3 jet matrix elements. The total cross section obtained at $\sqrt{s} = 1.8$TeV is $\sigma_{app} = 0.035 \pm 0.002$pb.

An alternative approximation method which has been proposed for W boson plus jets production[16] involves using the exact $W + 1$ jet matrix element as a starting point and adding extra jets by QCD bremsstrahlung in a parton shower cascade. This procedure works quite well in correctly reproducing the shapes of kinematical distributions over a wide range of energies. To reproduce the total cross section one needs to multiply by an ad hoc factor depending on the kinematical cuts.

5 Conclusions

We have suggested in this paper a simple and flexible set of approximations for W/Z plus jets production. these reproduce the shapes and normalizations of kinematical distributions at the $\sim 30\%$ level point-by-point in phase space and are an order of magnitude faster to numerically evaluate on a computer than the exact expressions. They can also be used to estimate as yet uncalculated processes such as $W + 5$ jet production as required. They should prove very useful in high statistics studies of backgrounds to $t\bar{t}$ and Higgs production at present and future hadron colliders.

6 Acknowledgements

C.J.M. would like to thank the Fermilab Theory group for hospitality during the period when this work was started. We also thank W. Giele for providing us with the code for the exact $W +$ jet matrix elements of ref. [1].

References

[1] F. A. Berends, H. Kuijf, B. Tausk and W. T. Giele, Fermilab-Pub-90/213-T (1990).

[2] K. Hagiwara and D. Zeppenfeld, Nucl. Phys. **B313** 560, (1989).

[3] R. Kleiss and W. J. Stirling, Phys. Lett. **200B** 193, (1988).

[4] C. J. Maxwell, Phys. Lett. **192B** 190, (1987).

[5] M. L. Mangano and S. J. Parke, Phys. Rev. **D39** 75, (1989).

[6] C. J. Maxwell, Nucl. Phys. **B316** 321, (1989).

[7] C. J. Maxwell, Phys. Lett. **225B** 425, (1989).

[8] G. Altarelli and G. Parisi, Nucl. Phys. **B126** 298, (1977).

[9] S. J. Parke and T. R. Taylor, Phys. Rev. Lett. **56** 2459, (1986).

[10] M. L. Mangano and S. J. Parke, Nucl. Phys. **B299** 673, (1988).

[11] F. A. Berends and W. T. Giele, Nucl. Phys. **B306** 759, (1988).

[12] M. L. Mangano, Nucl. Phys. **B309** 461, (1988).

[13] M. L. Mangano and S. J. Parke, Phys. Rep. **200** 301, (1991).

[14] W. T. Giele, D. A. Kosower and H. Kuijf, Fermilab-Conf-90/235-T (1990).

[15] A. D. Martin, R. G. Roberts and W. J. Stirling, Phys. Lett. **206B** 327, (1988).

[16] W. T.Giele, T. Matsuura, M. H. Seymour and B. R.Webber, Contribution to Proc. of "The 1990 Summer Study on High Energy Physics Research Directions for the Decade", Snowmass, CO. Fermilab-Conf-90/228-T (1990).

Figure 1: Comparisons of the exact (solid line) and approximate (points) histograms for W+4 jets, $W^{\pm}q\bar{q}'$ + gluons subprocesses, at $\sqrt{s}$ = 1.8 TeV. (a) E_T of jets, (b) jet pseudorapidity, (c) W transverse momentum, (d) W plus one jet mass, (e) W+ all jet mass, (f) all jet mass, distributions.

Figure 2: As Fig.1 but W+3 jets.

Figure 3: As Fig.1 but W+4 jet production, $W^{\pm}p\bar{p}'q\bar{q}$ + gluons subprocesses.

Figure 4: As Fig.1 but W+4 jets, all subprocesses.

Figure 5: W+5 jets production histograms approximated with one reduction (solid line) and two reductions (points). Other details as Fig.1.

Figure 6: Histograms for Z+4 jets approximated with one reduction, one and two $q\bar{q}$ subprocesses. Other details as Fig.1.

Cut Parameters	FNAL $p\bar{p}$ 1.8TeV	SSC pp 40TeV
E_T^{min} jet	15 GeV	50 GeV
$\lvert\eta_J^{max}\rvert$	2.0	3.0
ΔR_{JJ}^{min}	0.7	0.4
E_T^{min} leptons	20 GeV	50 GeV
$\lvert\eta_L^{max}\rvert$	1.0	3.0
ΔR_{JL}^{min}	0	0.4

Table 1: Kinematical cuts used at FNAL and SSC energies.

$W + 4j$ one $q\bar{q}$	FNAL $p\bar{p}$ 1.8TeV	SSC pp 40TeV
σ_{ex}	0.43±0.03 pb	35±3 pb
σ_{app}	0.41±0.02 pb	34±3 pb
f_{30}	0.73	0.72
f_{20}	0.55	0.57
f_{10}	0.31	0.35

Table 2: Comparison of the approximate and exact cross sections (σ_{ex}, σ_{app}) for W+4 jet production, $W^{\pm}q\bar{q}'$ + gluons subprocesses, at FNAL and SSC energies. Cuts as in Table 1. f30, f20, f10 denote the fraction of generated events passing the cut for which the approximation is within 30%, 20%, 10%, respectively, of the tree level result.

$W + 3j$ one $q\bar{q}$	FNAL $p\bar{p}$ 1.8TeV	SSC pp 40TeV
σ_{ex}	3.3±0.1 pb	76±10 pb
σ_{app}	2.6±0.1 pb	110±30 pb
f_{30}	0.60	0.56
f_{20}	0.43	0.42
f_{10}	0.24	0.25

Table 3: As for Table 2 but W+3 jet production.

$W + 4j$ two $q\bar{q}$	FNAL $p\bar{p}$ 1.8TeV	SSC pp 40TeV
σ_{ex}	0.25±0.01 pb	8.7±1.2pb
σ_{app}	0.20±0.01 pb	9.0±1.6pb
f_{30}	0.74	0.79
f_{20}	0.53	0.61
f_{10}	0.27	0.35

Table 4: As for Table 2 but for W+4 jet production, $W^{\pm}p\bar{p}'q\bar{q}$ + gluons subprocesses.

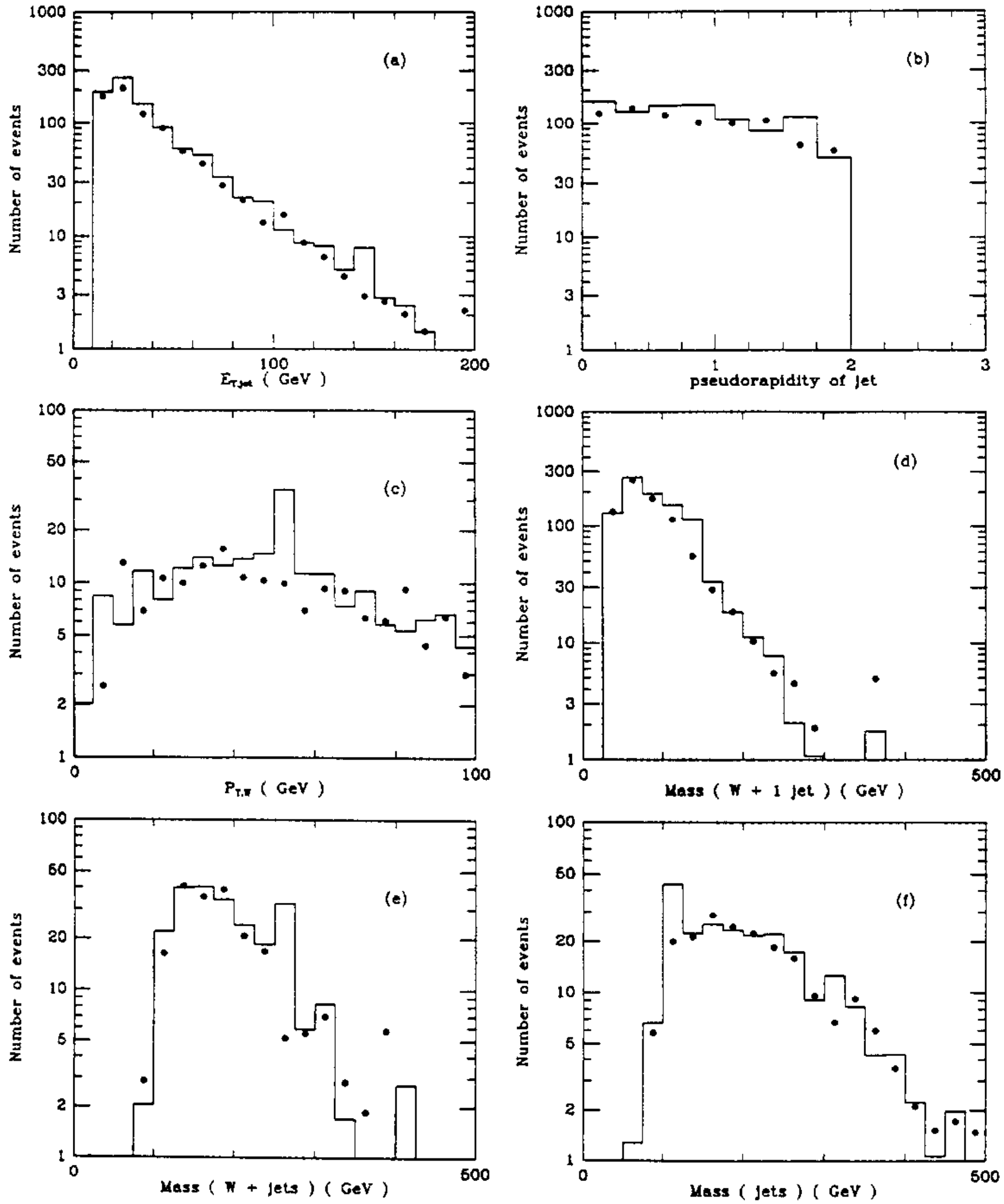

Figure 1: Comparisons of the exact (solid line) and approximate (points) histograms for W+4 jets, $W^{\pm}q\bar{q}'$ + gluons subprocesses, at $\sqrt{s}$ = 1.8 TeV. (a) E_T of jets, (b) jet pseudorapidity, (c) W transverse momentum, (d) W plus one jet mass, (e) W+ all jet mass, (f) all jet mass, distributions.

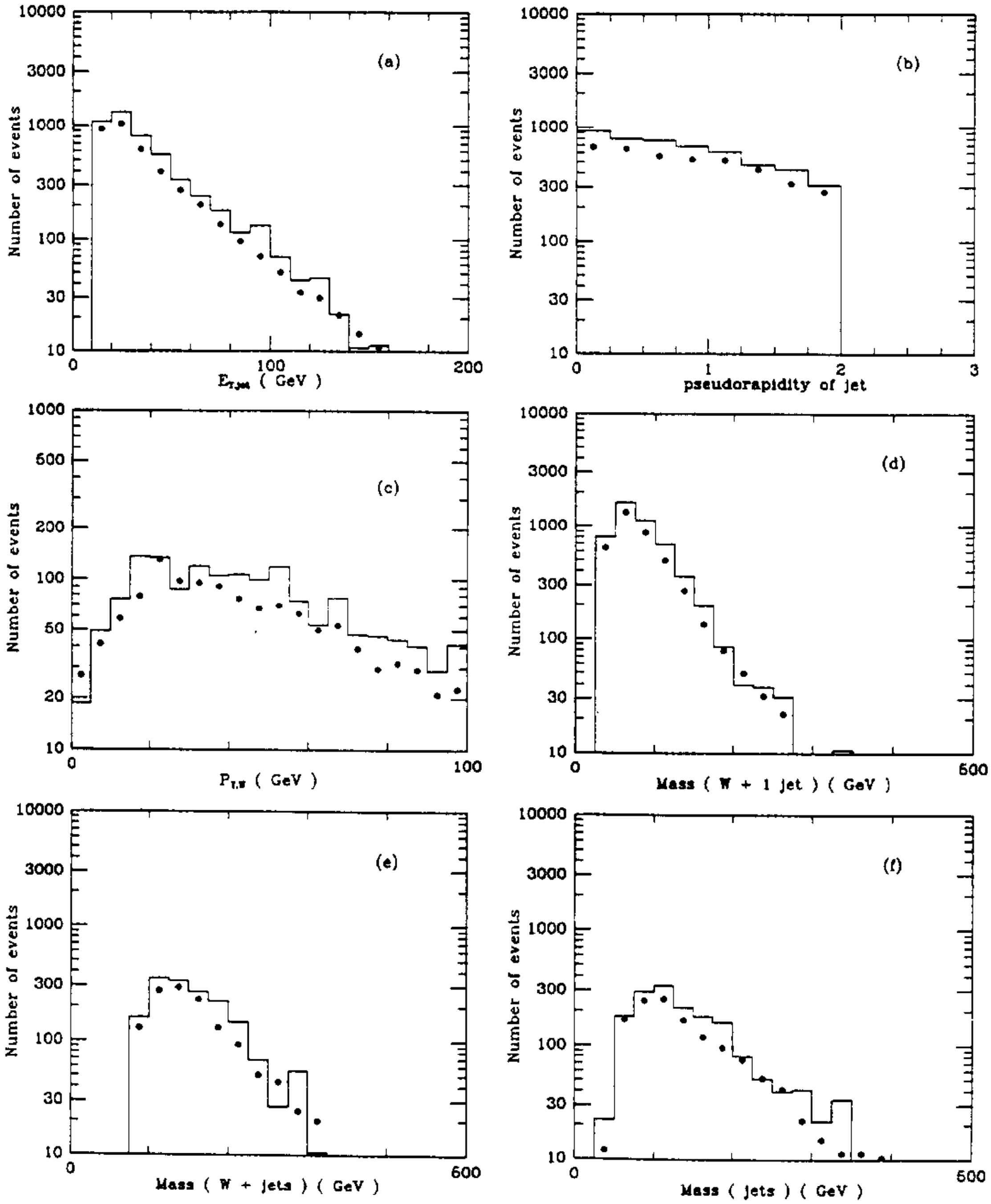

Figure 2: As Fig.1 but W+3 jets.

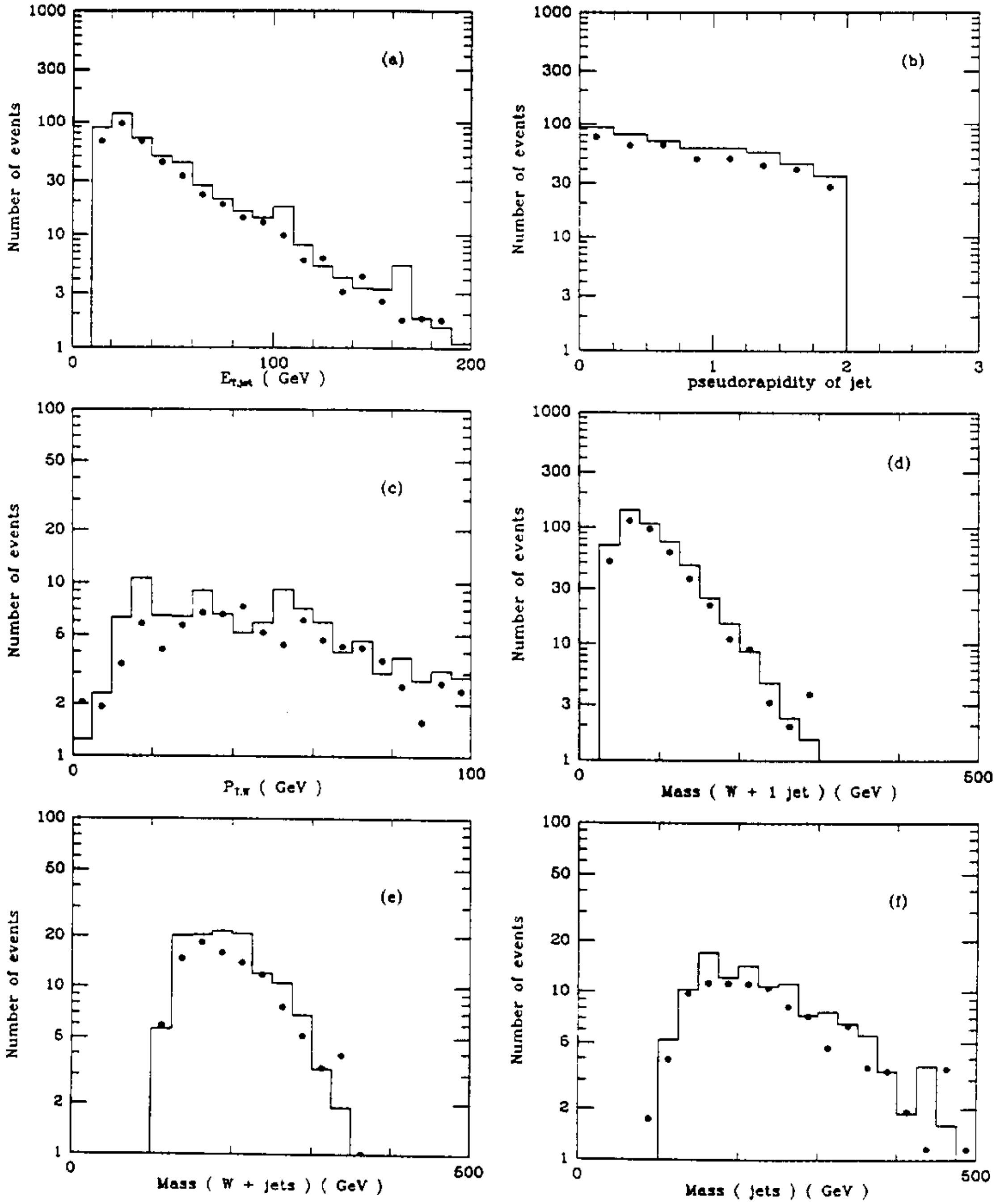

Figure 3: As Fig.1 but W+4 jet production, $W^{\pm}p\bar{p}'q\bar{q}$ + gluons subprocesses.

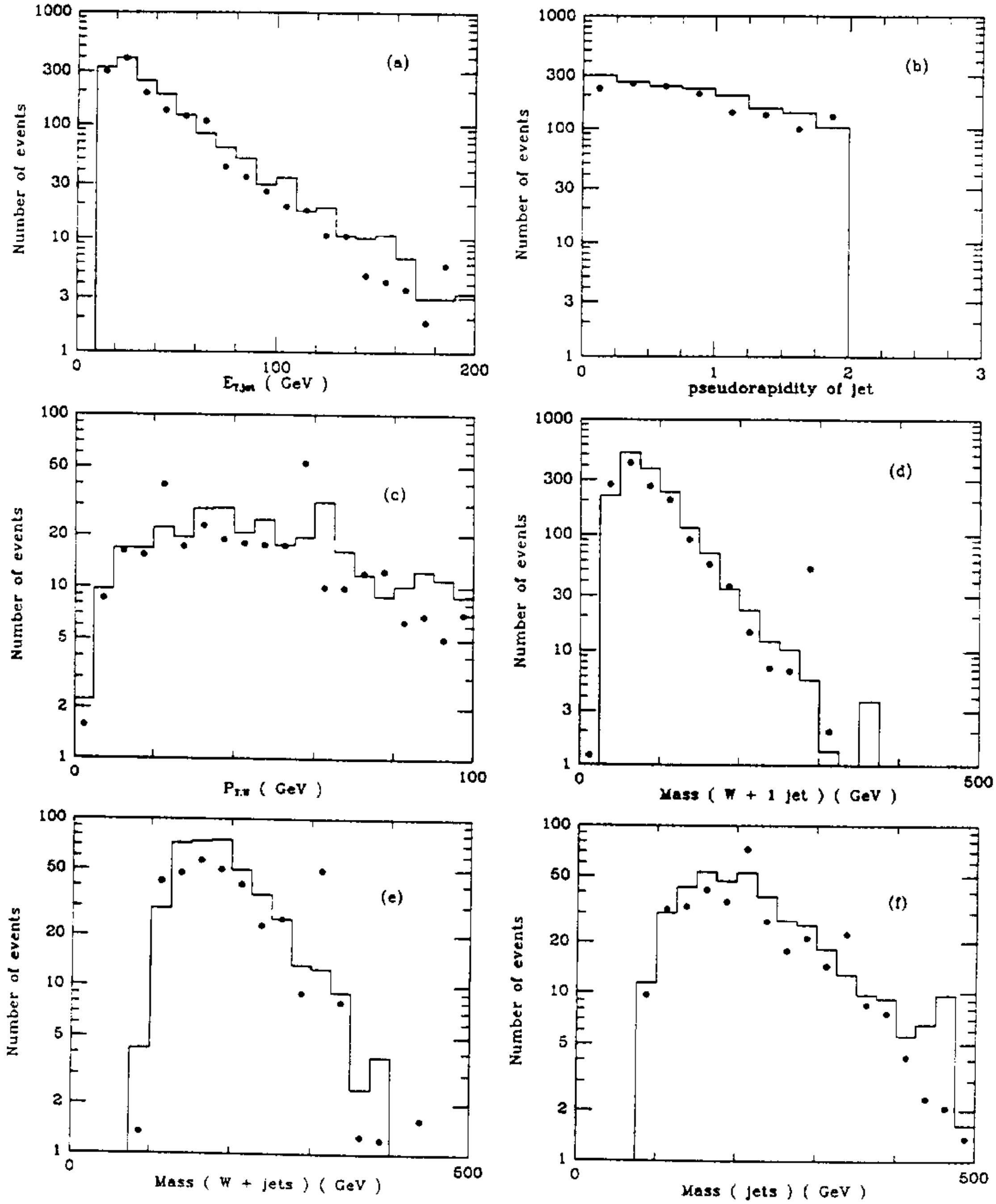

Figure 4: As Fig.1 but W+4 jets, all subprocesses.

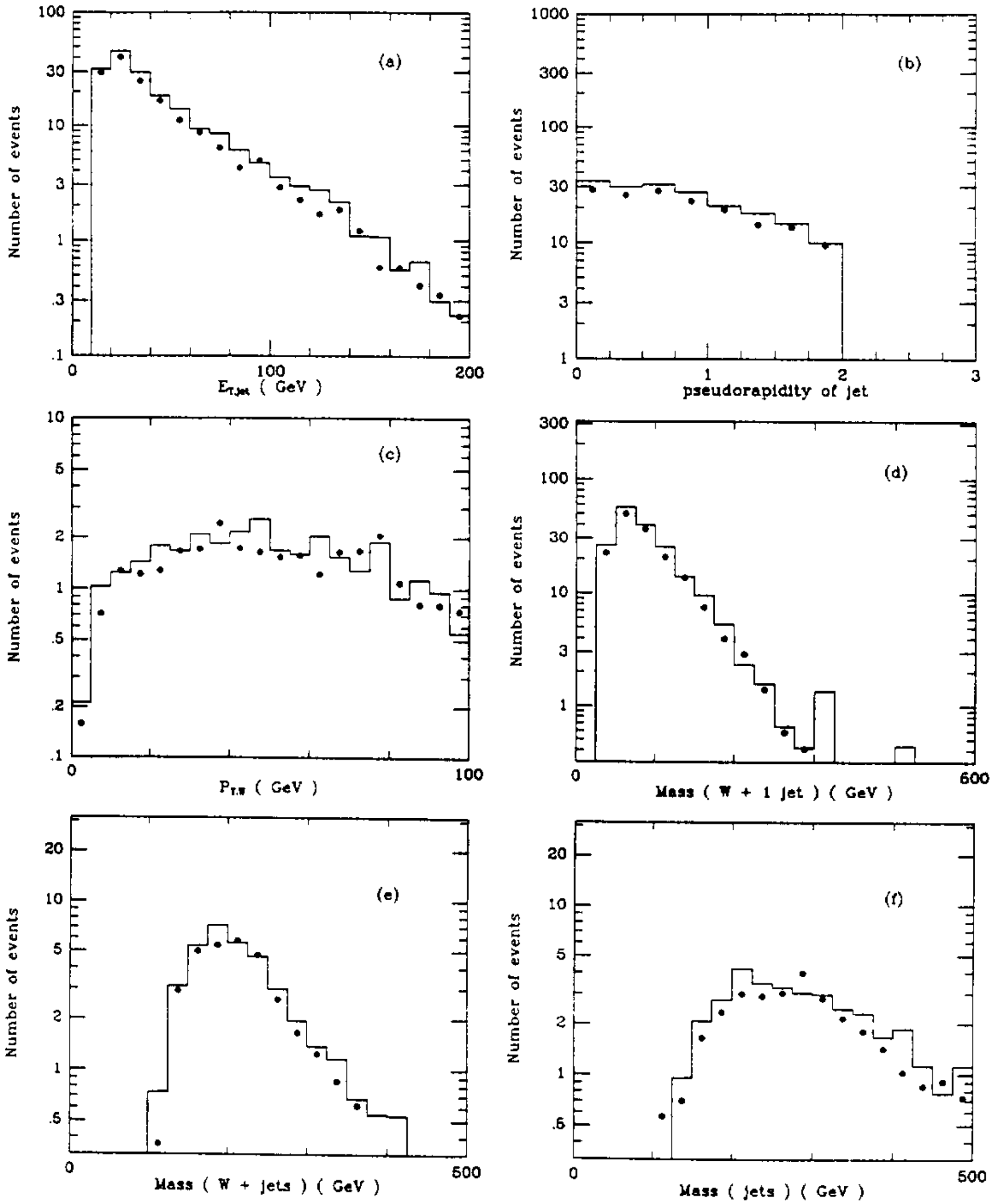

Figure 5: W+5 jets production histograms approximated with one reduction (solid line) and two reductions (points). Other details as Fig.1.

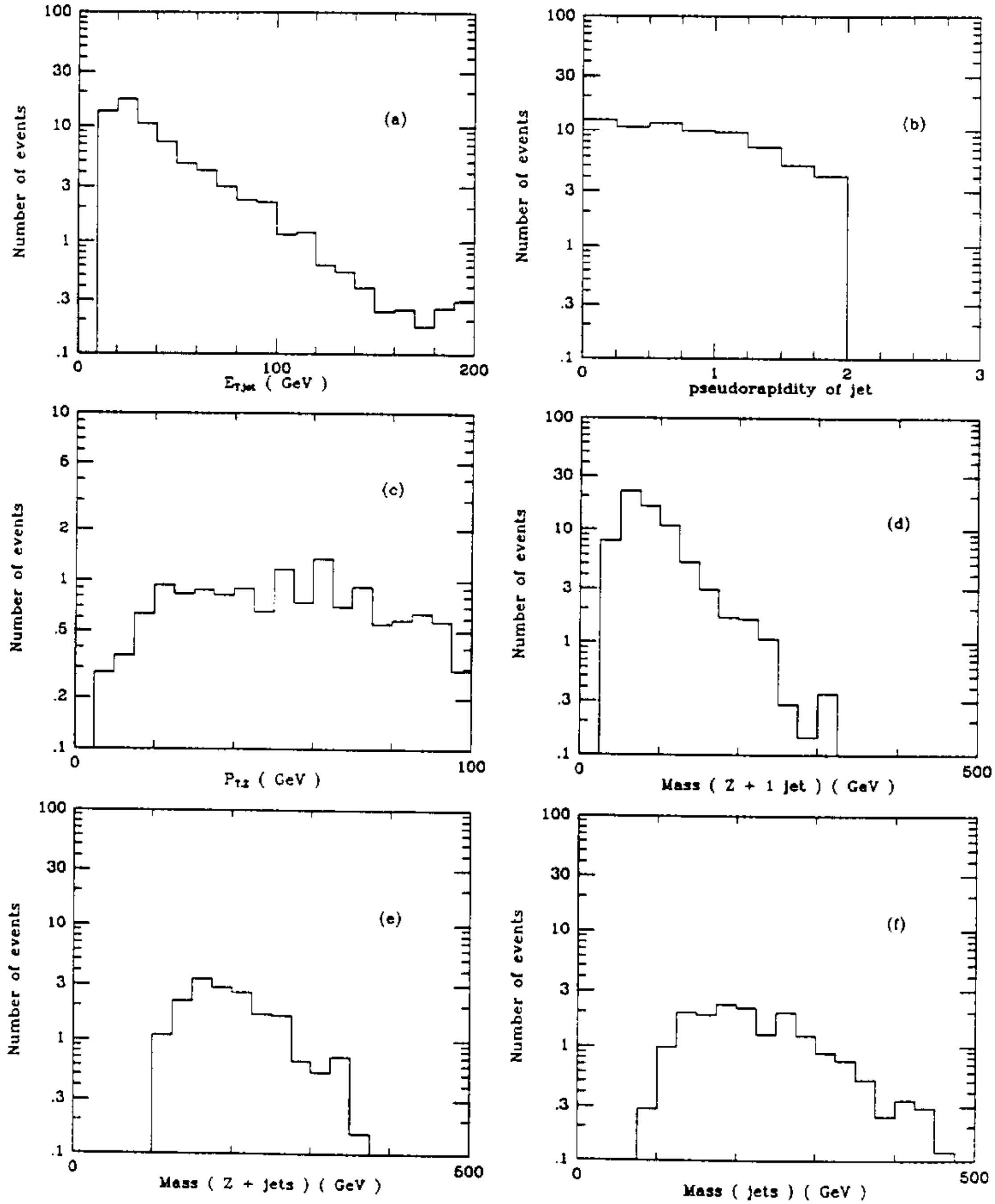

Figure 6: Histograms for Z+4 jets approximated with one reduction, one and two $q\bar{q}$ subprocesses. Other details as Fig.1.